1-to-12 surface normal three-dimensional optical interconnects

Ray T. Chen, Suning Tang, Maggie M. Li, David Gerald, and Srikanth Natarajan
Microelectronics Research Center, Department of Electrical and Chemical Engineering, University of Texas, Austin, Austin, Texas 78759

(Received 14 May 1993; accepted for publication 29 July 1993)

We present a surface normal optical interconnect with a 1-to-12 collinear fan-out. Two types of polymer-based holograms were fabricated to provide a collinear 1-to-12 fan-out from guided mode to substrate modes and twelve 1-to-1 surface normal interconnects. Fluctuation of up to 7.2 dB for the 1-to-12 fan-out hologram was observed due to the oscillating and the film saturation effects of the transmission hologram. Diffraction efficiency better than 70% was observed for all the total internal reflection holograms. The result reported herein greatly enhanced optical signal processing capability of guided wave optical interconnects. The advantages of free space optical interconnect, such as global interconnect, three dimension, massive fan-out/fan-in capabilities, and surface normal optical interconnect, can be realized using the demonstrated architecture. The coupling from waveguide to fiber can be realized from the surface rather than the edge of a photonic integrated circuit.

The intrinsic limitations of the current generation of computer have led researchers to seriously consider new computing architectures based on optical interconnects. The basic limitations of electrical interconnects include interconnection time bandwidths, clock skew, resistance-capacitance (RC) time constants, and even the distributed line resistance-inductance-capacitance (RLC) time consistent (for chip-to-chip interconnects and high level architecture). Fan-in and fan-out capabilities are also limited for electrical interconnections due to the electromagnetic wave interference and parasitic capacitance and inductance coupling. These difficulties associated with electrical interconnections are not solved by very-large-scale-integration (VLSI) technology.

Optical interconnect has been widely agreed as a better choice for interconnecting different processors and memories whenever the conventional electrical interconnect can not fulfill the system requirements. Among the optical interconnect architecture demonstrated thus far, free space multistage interconnect,[1,2] fiber-based interconnects,[3,4] and thin film polymer waveguide-based optical interconnects[5,6] represent the three major thrust areas. Multistage interconnects provide three dimension and thus a global interconnect scheme not achievable by guided wave optical interconnects. Optical fiber is low loss medium for point-to-point long distance interconnect (~ 1 to $\sim 10^6$). Thin film waveguide is the device of choice for two-dimensional intraplane interconnect where the waveguide routing pattern can be lithographically defined.

In this letter, we report, to our best knowledge, the first surface normal three-dimensional optical interconnect using a single-mode polymer waveguide in conjunction with a collinear waveguide hologram array. The polymer-based photonic integrated circuit employed for this demonstration is shown in Fig. 1 where the polymer-based multiplexed waveguide hologram is to convert the single-mode guided wave to substrate modes which are also guided within the substrate due to the total internal reflection effect. Formation of each predesigned waveguide hologram is to construct a grating vector such that a specific phase matching condition can be met. There are two different types of holograms involved in the surface normal optical interconnect. The first type (see Fig. 1) is to provide collinear diffraction from guided mode to substrate modes. There are 12 holograms recorded in the same emulsion area. The glass substrate we employed has a thickness of 1 mm and the separation between the two nearest surface normal beams is 2 mm. Each hologram has a bouncing angle Θ_i satisfying

$$\Theta_i = \tan^{-1}[i] \quad i = 1,2,3,4,5,6,7,8,9,10,11,12. \tag{1}$$

The phase-matching diagram is further detailed in Fig. 2, where the grating vector $K_i = \Lambda_i/2\pi$ for each substrate mode is clearly indicated. The holographic emulsion has an index of modulation as high as 0.2.[7] Therefore, a large number of gratings can be multiplexed onto the same emulsion areas.[8–10] The result reported herein represents the first 1-to-12 collinear fan-out in conjunction with surface normal coupling in a monolithically integrated polymer-based photonic integrated circuit.

In many situations, 1-to-many, many-to-1, and many-to-many interconnects are needed for many existing interconnect hierarchies such as mudule to mudule, backplane, and machine-to-machine interconnects. Holographic optical elements turn out to be one of the most promising tools

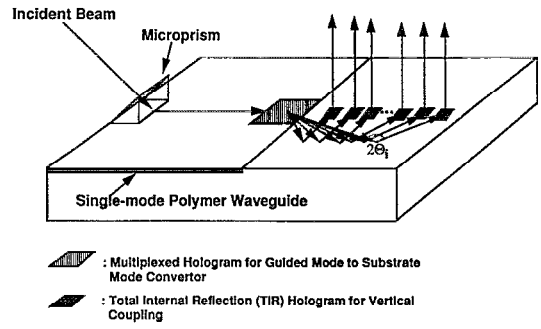

FIG. 1. Schematic of the polymer-based photonic integrated circuit for 1-to-12 surface normal optical interconnection.

 0003-6951/93/63(14)/1883/3/$6.00

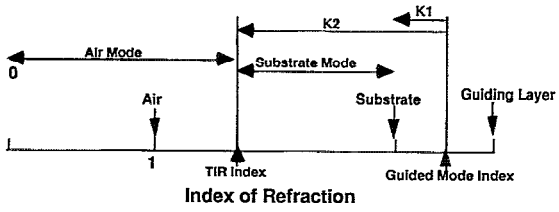

FIG. 2. Phase-matching diagram for the guided mode to substrate mode conversion: K_1 and K_2 are the minimum and maximum grating vectors for guided mode to substrate mode conversion.

to provide high fan-out capability. Tree and star couplers can only provide fan-out with small fan-out angles while holographic gratings can give us much larger fan-out angles (up to 2π). Therefore, the number of fan-outs and the angular dynamic range are much higher when using holographic gratings.

To construct the second type holographic grating (Fig. 1), the recording and reconstruction condition shown in Fig. 3 is required. Depending on the absorption characteristic of the holographic emulsion, proper recording beams need to be chosen. The holographic material has a strong absorption band at 488 nm which was chosen as the recording wavelength. The reconstruction wavelength is fixed at 632.8 nm which has a different wave vector and thus a different phase-matching condition for surface normal interconnect. The discrepancy for recording and reconstruction is clearly indicated in Fig. 3.

To form a slanted grating coupler which converts a substrate bouncing mode with bouncing angle Θ_i to a surface normal output beam (Figs. 1 and 3), the two incident angles of the recording beams (angles with respect to the waveguide surface) are

$$\theta_1=\sin^{-1}\left(\frac{n}{n_r}\sin(\delta)\right), \tag{2}$$

$$\theta_2=\sin^{-1}\left(\frac{n}{n_r}\sin(\Theta_i-\delta)\right), \tag{3}$$

where n is the index of refraction of the hologram and n_r is the refractive index of the medium on top of the hologram ($n_r=1$ for air) and

$$\delta=\frac{\Theta_i}{2}-\sin^{-1}\left[\frac{\lambda_b}{\lambda_r}\sin\left(\frac{\Theta_i}{2}\right)\right]. \tag{4}$$

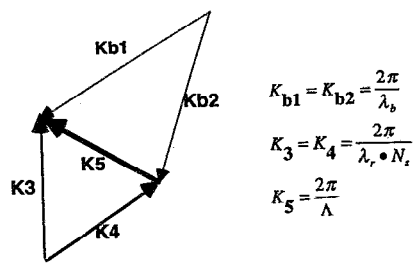

FIG. 3. Recording and reconstruction conditions for the total internal reflection hologram for the surface normal interconnects. λ_b=recording wavelength, λ_r=reconstruction wavelength, Λ=grating spacing, N_s =substrate index.

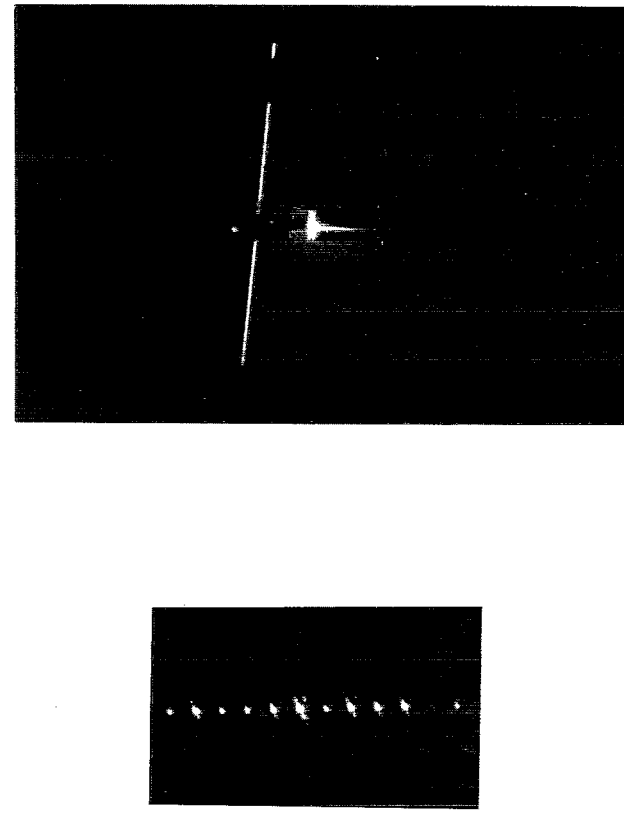

FIG. 4. (a) Reconstruction of the surface normal optical interconnect. Surface normal interconnection is not clear in this photograph due to the overlap between the diffracted beams and the undiffracted beam. (b) Near-field pattern of the 12 surface normal beams coupled out of the total internal reflection hologram array shown in Fig. 1. The separation between the two nearest beams is 2 mm.

In Eq. (4), λ_b and λ_r represent the wavelengths of the recording and the reconstruction beams, respectively. To increase angle Θ_i, i.e., increase the bouncing distance of the substrate mode (see Fig. 1), we can either decrease the ratio of λ_b/λ_r by changing the recording and reconstructing wavelengths or increase n_r by putting a high index prism right in front of the holographic emulsion areas in the recording process.

For the polymer-based photonic integrated circuit shown in Fig. 1, the total internal reflection (TIR) holograms are not multiplexed. Each hologram is to provide one surface normal beam for interconnect. As a result, the dynamic range of index modulation is very high. Furthermore, the second type hologram is reflection hologram with diffraction efficiency monotonically increased as the index modulation increases[12] while the first hologram is a transmission hologram with diffraction efficiency as an oscillating function of Δn. Thereby, the diffraction efficiency of the second type hologram is more controllable than the first type.

Reconstruction of the surface normal optical interconnect is shown in Fig. 4, where the polymer-based waveguide hologram with a 1-to-12 fan-out is not clearly seen in this photograph due to the overlap when observed at the surface normal direction. The undiffracted guided wave

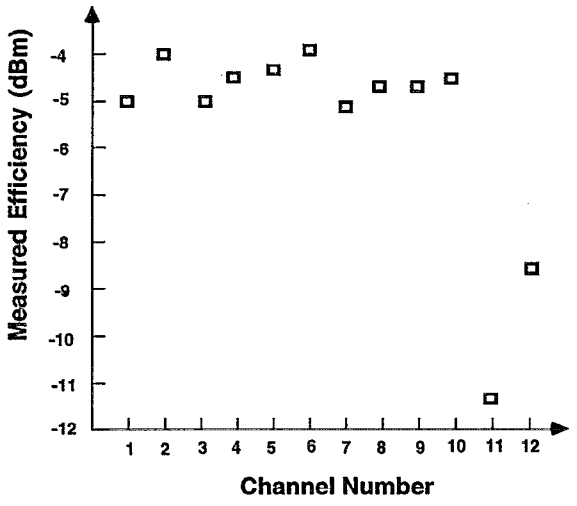

FIG. 5. Measured throughput intensity of the 12 surface normal beams. Power fluctuation of up to 7.2 dB is observed.

and the diffracted substrate waves were propagating collinearly and thus not distinguishable. The near field pattern of the 12 surface normal beams are displayed in Fig. 4(b) where the first ten fan-out channels have a relatively uniform intensity and the performance of the 11th and the 12th fan-out channels are relatively poor when compared with the first ten channels. The measured diffraction efficiency of these 12 fan-out beams is shown in Fig. 5. Variation of the first ten channels is within 1 dB while the last two channels have a deviation of 7.2 and 4.5 dB, respectively. This discrepancy is due to the oscillating effects of the holographic emulsion of the transmission hologram which provides the guided mode to substrate mode conversion. As far as the diffraction efficiency of the TIR hologram is concerned, the measured values of 12 holograms are all above 70% (not shown in this letter).

The result reported herein represents the first effort to eliminate the bottleneck of the two-dimensional nature of conventional thin film guided wave devices. The conversion of a guided mode to substrate modes provides the possibility of generating a reflection-mode multistage optical interconnects which fully take advantages of free space optical interconnects including global interconnect, three dimension, and massive fan-out/fan-in capability. Surface normal optical interconnect is provided through this demonstration. Availability of high speed surface emitting lasers,[13] flip-chip bonding technique and thin film liftoff devices[14] shall be the most desirable for surface normal integration. The demonstration reported in this letter automatically provides us with an optical clock signal distribution for backplane interconnect using synchronous bus protocol[15] when appropriate processor and memory boards are provided.

In summary, we present the first surface normal optical interconnect with a 1-to-12 collinear fan-out. Two types of waveguide holograms were fabricated to provide a collinear 1-to-12 guided mode to substrate mode fan-out and then 12-to-1 surface normal interconnects. Diffraction efficiency better than 70% was observed for all the total internal reflection holograms. Power fluctuation of up to 7.2 dB for the 1-to-12 fan-out hologram was observed due to the oscillating characteristic of the transmission hologram. The demonstrated result greatly enhanced the guided wave optical interconnects. The advantages of free space optical interconnect such as global interconnect, three dimension, massive fan-out/fan-in capabilities and surface normal optical interconnection can be realized using the reported technique.

This research is currently sponsored by Cray Research, Inc., Novex Corporation, Physical Optics Corporation, Army Research Office and the University of Texas at Austin.

[1] P. Guilfoyle, Proc. SPIE **1214**, 15 (1990; Critical Review Series, Digital Optical Computing, Vol. CR35, Los Angeles, CA, Jan. 16, 1990.
[2] H. S. Hinton, Proc. SPIE **1849**, 02 (1993).
[3] T. Lane, J. A. Quam, B. O. Kahle, and E. C. Parish, Proc. SPIE **1178**, 17 (1989).
[4] M. S. Cohen, M. F. Cina, E. Bassous, M. M. Oprysko, J. L. Speidell, F. J. Canora, Jr., and M. J. Defranza, *IEEE Conference on Components, Hybrids, Manufacturing Technology* (IEEE, New York, 1992), pp. 98–107.
[5] R. T. Chen, *Critical Review on Integrated Optics and Optoelectronics*, edited by K. K. Wong, (Society of Optical Engineering, 1993), pp. 268–306.
[6] R. T. Chen, Optics and Laser Technology, 1993 (invited review paper).
[7] R. T. Chen, W. Phillips, D. Pelka, and T. Jannson, Opt. Lett. **14**, 892 (1989).
[8] R. T. Chen, M. R. Wang, T. Jannson, Appl. Phys. Lett. **57**, 2071 (1990).
[9] R. T. Chen, H. Lu, D. Robinson, M. Wang, G. Savant, and T. Jannson, J. Lightwave Technol. **10**, 888 (1992).
[10] R. T. Chen, D. Robinson, H. Lu, M. R. Wang, and T. Jannson, Opt. Eng. **31**, 1098 (1992).
[11] R. T. Chen, M. R. Wang, G. Sonek, and T. Jannson, Opt. Eng. **30**, 622 (1991).
[12] H. Kogelink, Bell Syst. Tech. J. **48**, 2909 (1969).
[13] J. Ma, B. Catanzaro, W. Daschner, Y. Fainman, and S. H. Lee, Proc. SPIE **1849**, 18 (1993).
[14] E. Yablonovitch, D. M. Huang, T. J. Gmitter, L. T. Florez, and J. P. Harbison, Appl. Phys. Lett. **56**, 2419 (1990).
[15] R. T. Chen, Proc. SPIE **1849**, 25 (1993).